CrystEngComm

Accepted Manuscript

This is an *Accepted Manuscript*, which has been through the Royal Society of Chemistry peer review process and has been accepted for publication.

Accepted Manuscripts are published online shortly after acceptance, before technical editing, formatting and proof reading. Using this free service, authors can make their results available to the community, in citable form, before we publish the edited article. We will replace this *Accepted Manuscript* with the edited and formatted *Advance Article* as soon as it is available.

You can find more information about *Accepted Manuscripts* in the Information for Authors.

Please note that technical editing may introduce minor changes to the text and/or graphics, which may alter content. The journal's standard Terms & Conditions and the Ethical guidelines still apply. In no event shall the Royal Society of Chemistry be held responsible for any errors or omissions in this *Accepted Manuscript* or any consequences arising from the use of any information it contains.

ROYAL SOCIETY
OF CHEMISTRY

www.rsc.org/crystengcomm

Journal Name

ARTICLE

In-situ monitoring the role of citrate in chemical bath deposition of PbS thin films

Received 00th January 20xx,
Accepted 00th January 20xx

DOI: 10.1039/x0xx00000x

www.rsc.org/

Sucheta Sengupta[a], Maayan Perez[a], Alexander Rabkin[a] and Yuval Golan[a]*

Tri sodium citrate (citrate) has been commonly used as a co-complexing agent during chemical bath deposition to improve film quality and control grain size, yet its precise role has not been elucidated to date. In this study, we have focused on the role of citrate in chemically deposited PbS thin films. Citrate effectively complexes the lead cation in solution thereby decreasing growth rate and inducing growth in the cluster mechanism. This was monitored in real time using laser light-scattering and UV-Vis absorption spectroscopy which quantitatively confirmed the retarded PbS formation in the cluster mechanism in presence of citrate. Nanocrystalline PbS films formed in presence of citrate show quantum confinement effects with blue shifted optical properties compared to the bulk, adding an important path for controlling film properties towards future infrared optoelectronic applications.

Introduction

Chemical bath deposition (CD) is by far the most cost effective method for reproducibly producing high quality semiconductor thin films[1]. Early studies focused on deposition of lead chalcogenide (PbS, PbSe) thin films by CD due to their technological importance as infrared radiation detectors and emitters predicted as early as 1904[2,3]. Particularly, lead sulfide (PbS) have been subject to considerable research due to its direct narrow bandgap energy (0.41 eV) and large exciton Bohr radius (18 nm) and useful optoelectronic properties for infrared detection and emission[4-6]. Deposition of thin PbS films on GaAs provides the means for integration of PbS IR optoelectronics with GaAs based technology.

We have previously showed that control over the microstructure of PbS thin films on GaAs (100) can be achieved by optimizing the deposition time, deposition temperature and the concentrations of the reactants present in the bath[7-9]. PbS was deposited from an highly alkaline aqueous solution where the NaOH besides affecting the rate of thiourea decomposition, also effectively complexes the Pb^{2+} metal ions. Tri sodium citrate (citrate) has been commonly used as a co-complexing agent during CD especially for metal cations such as zinc (Zn^{2+}) an tin (Sn^{2+}) to produce high quality films with better uniformity and decrease in the grain size[10,11]. In the particular case of PbS, it was observed that an increase in the concentration of citrate resulted in increased film uniformity and decrease in the crystallize size with the citrate ions being present as the functional group in the PbS film [12-14]. In presence of citrate, the hydroxyl citrate complex of Pb $[Pb(OH)(cit)]^{2-}$ (with variable co-ordination number depending on the pH of the solution[15]) would be expected to decompose differently from the common Pb-hydroxide complex. Thus, it would be important to study the effect of the co-complexant on film growth which can provide control over growth mechanism and result in different film morphologies and physical properties.

The mechanism involved in the CD process is quite intriguing and holds the key for controlling film morphology. Generally, the role of the complexing agent is to bind with the metal ions to prevent rapid reaction and precipitation of the metal hydroxide; hence, in the absence of a complexant there is excessive and rapid precipitation with little or no film formation. The metal complex allows the slow release of the free metal ion to react with the slowly generated anion (usually formed by the controlled hydrolysis of the precursor) directly onto the substrate, the process commonly known as the ion-by-ion mechanism. Alternatively, the film growth can also occur by migration and adsorption of colloidal particles either of the metal chalcogenide, the metal hydroxide or of insoluble metal complexes generated in the solution onto the substrate, the process commonly known as the cluster mechanism. The change in the mechanism is manifested in a shift from the formation of a highly oriented monocrystalline film to a nano-crystalline cluster. Hodes *et al.* have previously demonstrated that this changeover in the mechanism can be affected by the change in the metal-complex ratio[16,17]. They described that there is a particular critical ratio (R_c) between the complexing agent and the metal ions below which the cluster mechanism is dominant which can be related to the

---

[a] *Department of Materials Engineering, and the Ilse Katz Institute for Nanoscale Science and Technology, Ben-Gurion University of the Negev, Beer-Sheva 84105, Israel.*

Electronic Supplementary Information (ESI) available: [details of any supplementary information available should be included here]. See DOI: 10.1039/x0xx00000x

CrystEngComm Accepted Manuscript

Please do not adjust margins

presence of metal-hydroxide, and above it, one has the direct deposition of the film onto the substrate through ion-by-ion mechanism. The range of R_c could be more accurately defined in the case of CdSe than compared to PbSe since PbSe was always found to form in the solution under all the experimental conditions. Notably, under the same conditions, PbS was always found to form directly onto the substrate. This change in the behavior can be rationalized by comparing the solubility product of the different chalcogenides formed which decreases in the order PbS>CdSe>PbSe and hence the nucleation of PbSe occurs at much lower concentrations in the solution than would be required for equivalent formation of either CdSe or PbS.

Despite the critical role of the citrate as a complexing agent in CD, its exact role in affecting film growth has rarely been systematically studied. The present work elucidates the two opposingrole of citrate depending on the active mechanism involved. Using *in-situ* light scattering and optical absorbance spectroscopy, we have monitored the deposition solutions during the early stages of the film growth. Combined with ex-situ characterization of the resulting thin films, we show that citrate has a unique and well-defined effect depending on the active growth mechanism.

Experimental

2.1 Materials and methods

PbS thin films were deposited from solutions containing $Pb(NO_3)_2$, $CS(NH_2)_2$, $Na_3C_6H_5O_7$ and NaOH at two different temperatures. Thiourea (TU) (Aldrich, ACS≥ 99.0%), lead nitrate (Aldrich, analytical 99.99+%), trisodium citrate (referred to here as 'citrate') (Aldrich) and sodium hydroxide (Aldrich, reagent grade≥98% pellets, anhydrous) were used without further purification. Distilled water was obtained from a Millipore Direct Q3. The deposition temperature was fixed at 20° and 30°C. The deposition solutions were prepared by adding NaOH, citrate and lead nitrate in this particular order. Before the addition of TU, the last reagent, the solutions were purged with pure N_2 gas for 60 min in order to reduce levels of dissolved O_2 and CO_2. Single side polished, undoped GaAs (100) were purchased from AXT Inc. The wafers were cleaved into 2 cm*1 cm samples, cleaned with ethanol and water and passivated for 10 min in the deposition solution prior to the deposition. Typically, the deposition was carried for 120 min at a particular temperature within a thermostat. The resultant film morphology was studied by X-ray diffraction (XRD) and ultrahigh resolution scanning electron microscopy (UHR-SEM). For *in-situ* measurements, the growth solutions (except for TU) were purged and thermally equilibrated for 5 min before initiating the reaction by adding the last reagent, the point from where real time monitoring was carried out using laser light scattering and UV-vis spectroscopy.

2.2 Characterization Method

2.2.1 X-Ray diffraction (XRD)

The phase and orientation of the films were studied by XRD. A Rigaku Model 2000 diffractometer operating in the θ/2θ geometry using Cu Kα radiation (λ = 1.5405 Å) was used at 40 kV and 30 mA. Scans were obtained in a 2θ range of 20-60° in 0.02° steps.

2.2.2 High resolution scanning electron microscopy (HRSEM)

The morphology of the films was observed using an ultrahigh resolution JEOL JSM-7400F field emission gun (FEG)-SEM without coating of the surface. Acceleration voltage was fixed at 3.5 kV. Film thickness was measured from cross sections and surface topography was observed in plan-view.

2.2.3 Light scattering (LS)

Scattering spectra were collected by using CSG-3 (ALV, Langen, Germany). The laser power was 20 mW at the He-Ne laser line (632.8 nm). Averaged scattered intensities were measured by ALV/LSE 5004 multiple tau digital cross correlator, at scattering angles of 30-90° at 20° and 30°C temperatures as a function of time. The scattering intensities were normalized with respect to blank solvent (viz. water and toluene).

2.2.4 Optical properties

UV-vis spectra were obtained *in-situ* from the deposition solutions using a Hewlett-Packard 8453 diode array spectrophotometer equipped with a cell temperature controller. PL were measured using Bruker VERTEX 80v FT-IR spectrometer, equipped with a PL module with a 100 mW 785 nm excitation laser.

Results and discussion

The effect of citrate concentration on the microstructure of PbS films chemically deposited on GaAs (100) for 120 min at a temperature of 20°C was studied using XRD (Figure 1). The diffractogram in Figure 1a corresponds to a PbS film grown at 20°C in absence of citrate. Figures 1b-d corresponds to films grown at 20°C with three different concentrations of citrate, 4.25 mM, 8.5 mM and 17 mM. The XRD patterns indicate that the introduction of citrate in the deposition solution induces prominent texturing in the (100) direction. Interestingly, this texturing is observed for the lowest concentration of citrate and thereafter increasing the concentrations has little effect on the film texture. The HRSEM images (Figure 1 e-h) show that the films deposited in presence of citrate are comprised of highly oriented cube-shaped ~80-100 nm grains compared to the randomly oriented grains observed in absence of the citrate. Another prominent observation is the drastic reduction in the grain size in presence of citrate. These cube-shaped

CrystEngComm Accepted Manuscript

This journal is © The Royal Society of Chemistry 20xx

grains are formed as the preferred morphology for all citrate concentrations.

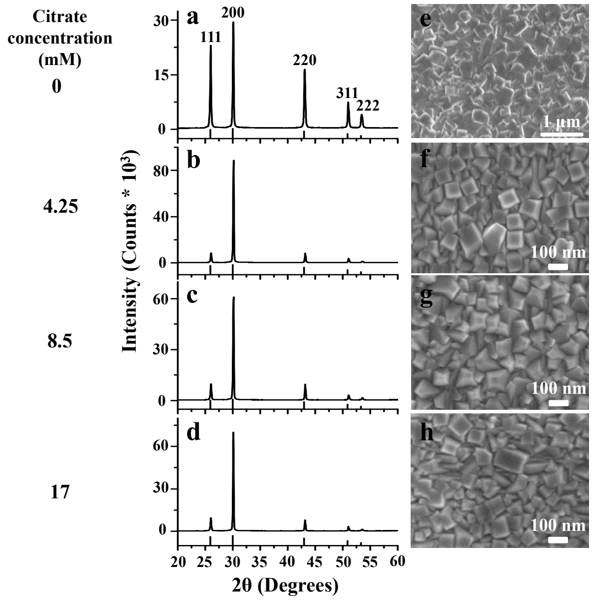

Figure 1. (a-d) XRD patterns for films grown at 20°C for 120 min with different concentrations of citrate, 0 mM, 4.25 mM, 8.5 mM and 17 mM, respectively. (e-h) Corresponding plan-view HRSEM images.

This trend in orientation can be quantitatively evaluated by plotting the diffracted intensity ratio $I_{(200)}/I_{(220)}$ as a function of citrate concentration (Figure 2a). In presence of citrate, this ratio increases from powder ratio (randomly oriented grains) in the 0 mM citrate sample to about 6 for all three concentrations, reflecting the prominent (100) texture. The film thickness values were estimated from cross sectional HRSEM images and plotted as a function of citrate concentration (Figure 2b). In presence of the citrate, the film thickness is drastically reduced compared to the blank. With increasing citrate, the film thickness slightly decreases further. In agreement with the film thickness variation, the integrated area of the XRD spectra similarly decreases with increasing citrate concentration.

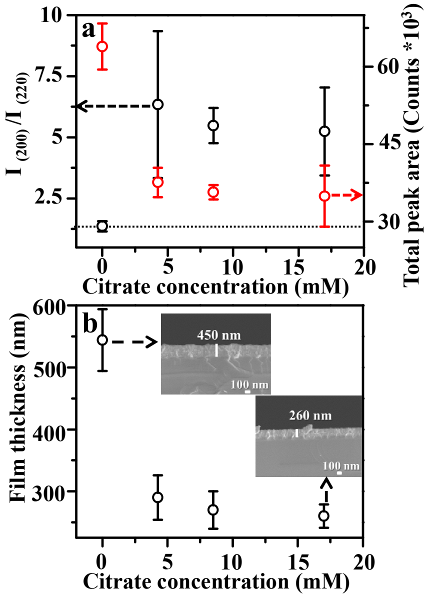

Figure 2. Effect of citrate concentration for PbS films grown at 20°C for 120 min (a) $I_{(200)}/I_{(220)}$ Bragg peak intensity ratio (black) and total peak area (red). The dotted line indicates the powder ratio. (b) Film thickness observed from cross-sectional HRSEM images.

Next, the deposition temperature was increased to 30°C. The resultant XRD diffractograms for the films grown for 120 min at 30°C with different citrate concentrations are described in Figure 3 (a-d). At 30°C, without citrate, the resultant PbS thin film has a strong (110) texture as previously reported in the literature (Figure 3a), [7,9] while there is a gradual increase of the (200) Bragg peak with increasing citrate concentration. The corresponding plan-view HRSEM images are described in Figure 3 (e-h). For films deposited in the presence of citrate, the HRSEM images show the formation of cube-shaped grains with increasing citrate concentrations along with the presence of rectangular pyramidal topography that is typical for <110> oriented films. Though the cube-shaped grains are formed for the highest citrate concentration at both the temperatures, it is important to note that the grain size is increased quite significantly with temperature.

CrystEngComm Accepted Manuscript

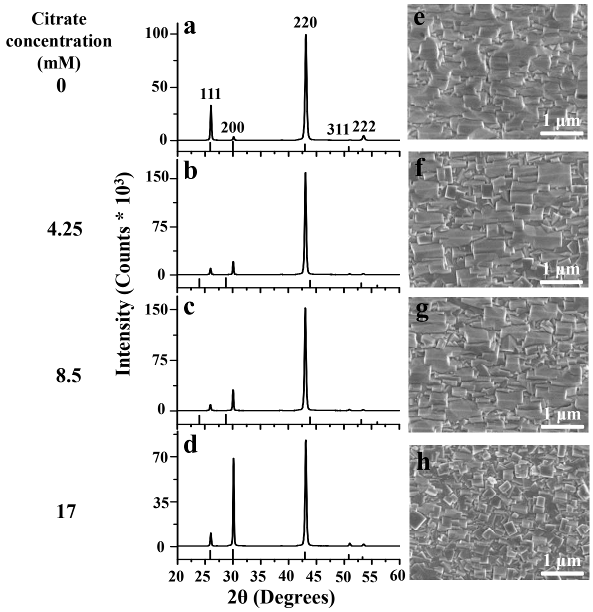

Figure 3. (a-d) XRD patterns for films grown at 30°C for 120 min with different concentrations of citrate, 0 mM, 4.25 mM, 8.5 mM and 17 mM. (e-h) Corresponding plan-view HRSEM images.

This increase in the preferred texturing can be quantified by plotting the ratio of Bragg peak intensities $I_{(200)}/I_{(220)}$ as a function of citrate concentration (Figure 4a). With increasing citrate concentration, the intensity ratio increases and approaches the powder ratio value from highly (110) oriented film in case of the blank. When the film thickness is plotted as a function of citrate concentration, it is found to initially increase compared to the blank and then remain more-or-less constant with further increase in citrate concentration (Figure 4b). The same trend was also observed, as expected, for the integrated peak area of the XRD spectra vs. citrate concentration. Interestingly, with the highest citrate concentration, though the film thickness increases from the blank, the total integrated peak area as calculated from the XRD spectrum decreases. This may suggest formation of amorphous clusters resulting from parallel growth of cluster mechanism along with the dominant ion-by-ion mechanism induced by the presence of citrate.

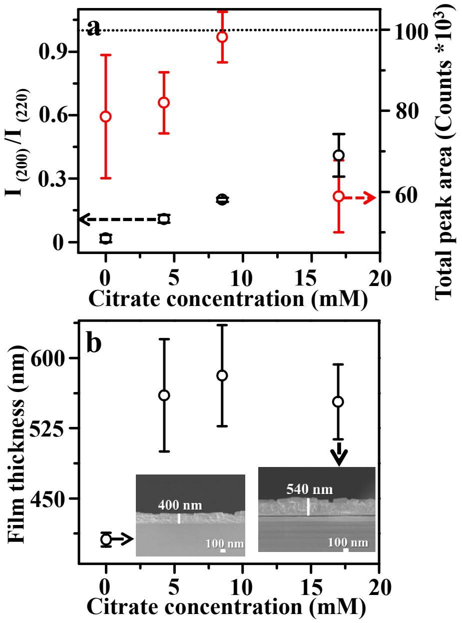

Figure 4. Effect of citrate concentration for PbS films grown at 30°C for 120 min (a) I(200)/I(220) Bragg peak intensity ratio (black) and total peak area (red). The dotted line indicates the powder ratio. (b) Film thickness observed from the cross sectional HRSEM images.

Apart from varying the growth temperature, we have studied the effect of pH of the growth solution at both the temperatures. At 20°C, at pH 12.9 and 13.2 randomly oriented PbS grains are formed (Figure 5 a, b) in absence of citrate. In presence of citrate, cube shaped grains are formed in both pH values with the average dimensions increasing with pH from ~20-50 nm to ~100 nm (Figure 5 d,e). Upon increasing the pH further to 13.4, both in presence and in absence of citrate, the resultant film morphology is composed of rectangular pyramidal topography (Figure 5 c,f) typical of ion-by-ion growth mechanism.

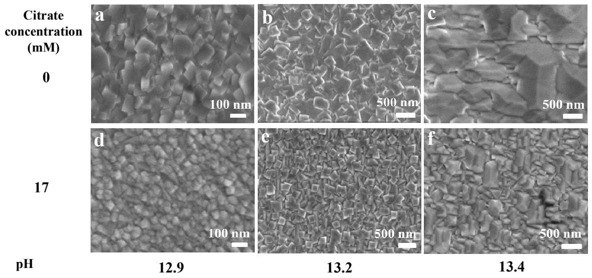

Figure 5. Plan-view HRSEM images of samples deposited at 20°C for 120 min with three different pH values (a-c) 0 mM citrate (d-f) 17 mM citrate.

CrystEngComm Accepted Manuscript

The same trend is observed at a deposition temperature of 30°C (Figure 6). At pH 12.9 presence of citrate results in the formation of nanoscale spherical particles. At pH 13.2, cube-like grains are formed in presence of citrate and with further increase in pH to 13.4; presence of the citrate has little effect on the orientation of the film.

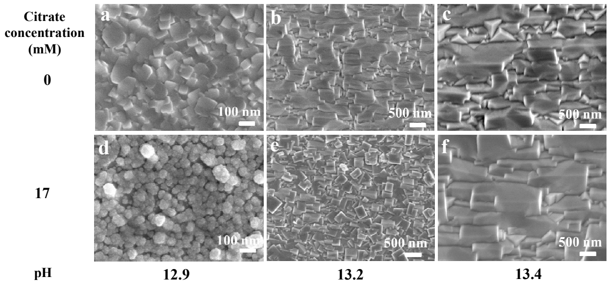

Figure 6. Plan-view HRSEM images of samples deposited at 30°C for 120 min with three different pH values (a-c) 0 mM citrate (d-f) 17 mM citrate.

The variation in film thickness vs. pH at both temperatures is presented in Figure 7. From the plots it is evident that there is a transition between the two active deposition mechanisms with the change in temperature and pH. Citrate is found to have opposing effect on the two deposition mechanism. While it retards the film growth in the case of cluster mechanism, for ion-by-ion mechanism the film thickness increases in presence of citrate. Interestingly, the transition between the two mechanisms was found to shift to lower pH value with increasing temperature, at 20°C the pH for the transition was found to be 13.2 which decreases to <13.1 at 30°C.

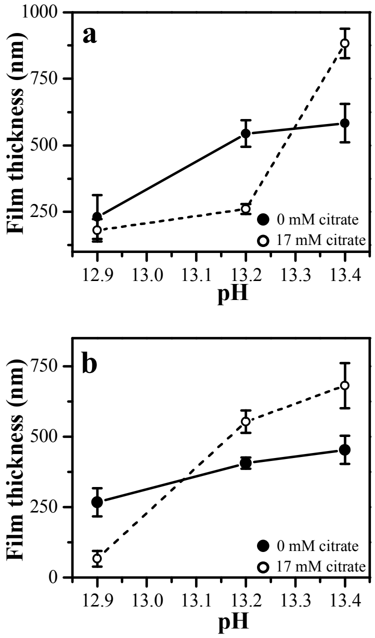

Figure 7. Film thickness plotted vs. pH for 0 mM and 17 mM citrate (dashed and solid lines, respectively) for two deposition temperatures (a) 20°C and (b) 30°C.

From the above results, it is evident that the citrate affects the growth of PbS in two completely different ways depending on the active deposition mechanism. It has been previously shown that the observed changes in film morphology upon changing the temperature or pH occur due to a transition in the active deposition mechanism[1]. As discussed earlier, there are primarily two main mechanisms that are active in CD, cluster mechanism and ion-by-ion mechanism. It has been shown earlier that these two mechanisms result in distinct film morphologies and can easily be identified using laser light scattering (LS)[18]. The cluster mechanism gives rise to high scattering intensities which strongly depend on the particle size and particle concentration present in the solution. On the other hand, the scattering intensity sharply decreases once the clusters settle and the deposition proceeds via transition to the ion-by-ion mechanism. Thus using LS one can effectively determines the transition point between the mechanisms which can be further correlated with the structural characterization of the films obtained from time interrupted growth series[18].

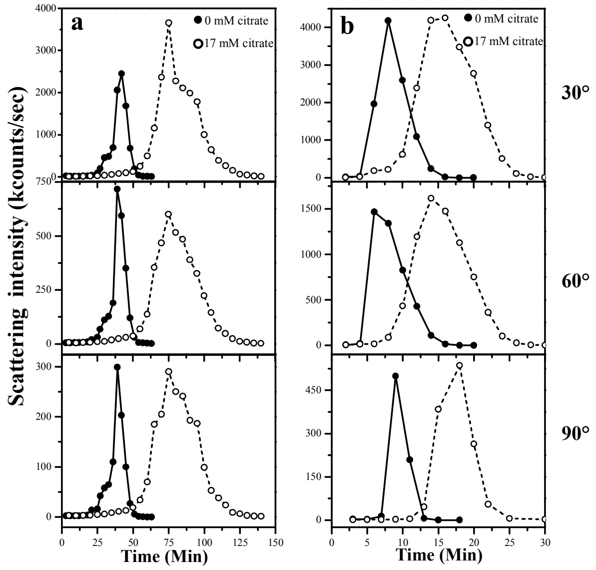

Figure 8. Time resolved LS data obtained at three different temperatures (a) 20°C (b) 30°C at three different scattering angles θ=30°, 60° and 90° showing the deposition mechanism transition point with (17 mM), and without (0 mM) citrate as denoted by dashed and solid lines, respectively.

In-situ LS measurements have been performed for the deposition solutions at 20°C and 30°C both in absence and presence of citrate, and are shown in Figure 8. It is seen that at the beginning of the reaction, the scattering intensity increases sharply indicating initiation of deposition in the cluster mechanism, where clusters are formed during the initial stages of the reaction giving rise to strong scattering intensity.

CrystEngComm Accepted Manuscript

Subsequently, upon increasing the reaction time, most particles settle down and the solution becomes transparent to light indicating a transition to an active ion-by-ion mechanism. In absence of citrate at 20°C, this transition time is found to be in the interval of 30-45 min after the reaction commences. However, in presence of citrate, this transition is substantially slowed down and it now occurs in the time interval range of 75-120 min after the commencement of the reaction. Interestingly, not only the onset of the reaction is delayed but the FWHM (full-width-half-maxima) of the curves also increases from ~9 min (in blank) to ~20 min in presence of citrate. On increasing the temperature to 30°C, we see the same effect but at a much smaller time scale. Without citrate, there is initial formation of clusters which rapidly settle within 8-15 min. In presence of citrate, the initial cluster formation is somewhat bit delayed with the transition now occurring within 15-25 min. At this temperature also, the FWHM of the curves increases from ~4 min (in blank) to ~10 min in presence of citrate. Thus, the LS results indicate that the presence of citrate in the deposition solution results in a much delayed transition from cluster to ion-by-ion mechanism at both the temperatures.

It has previously been reported that in a polydispersed solution, the scattering intensity depends on the size of the particles and thus at low scattering angles most scattered light comes from the large particles and at higher angles most scattered light comes from the smaller particles[19]. While at higher temperature, 30°C, there is not much of a difference in the scattering intensities with the presence of citrate, at 20°C the scattering intensity at the lower angle is much higher in the presence of citrate compared to the blank. In presence of citrate, due to the chelating effect, it can presumably bind to more than one metal ion to form larger, chain-like clusters increasing the extent of Pb^{2+} complexation and slowing the rate of the complex decomposition and hence delaying the formation of the PbS film via the cluster mechanism. Once the mechanism switches to ion-by-ion mechanism at higher temperature, the complex directly and rapidly decomposes on the substrate and hence the presence of citrate has little effect on the rate of the PbS film formation and on the resulting film morphology.

To verify this assumption, an interrupted growth series of chemically deposited PbS films in presence and absence of citrate was deposited on GaAs (100) with growth terminated after 5, 15 and 30 min. The resulting samples were studied using plan-view HRSEM and the results are depicted in Figure 9. As LS data suggested, at 20°C, 5 min after the initiation of the reaction, there is no sign of nucleation for both with and without citrate. However, in absence of citrate, film growth started after 15 min with uniform PbS nucleation which grows to form bigger grains with time, while in presence of citrate, the commencement of the reaction is drastically retarded with very small signs of nucleation showing up only after 15 min of reaction, and resulting in non-uniform coverage.

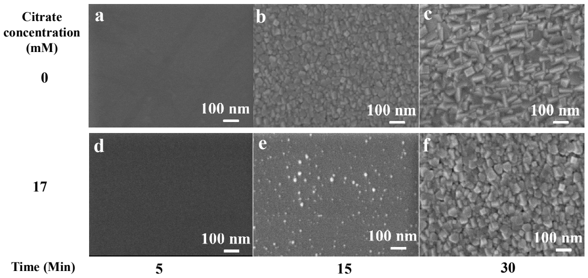

Figure 9. HRSEM plan-view images showing a time interrupted growth series of PbS films deposited at 20°C for 5, 15 and 30 min from the initiation of the reaction in presence of (a-c) 0 mM and (d-f) 17 mM citrate.

For a deposition temperature of 30°C, uniform nucleation is seen already after 5 min in the absence of citrate, which rapidly grows to larger crystallite size with time (Figure 10 a-c). In presence of citrate, the nucleation is somewhat delayed with a uniform film forming only after 15 min of reaction (Figure 10 d-f). In general, addition of citrate slows down the reaction, manifested by slower nucleation on the GaAs substrates. This observation is in well agreement with the data obtained from the LS experiments.

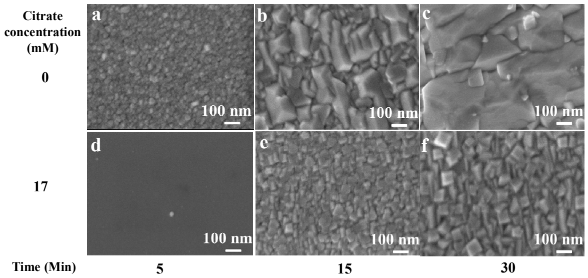

Figure 10. HRSEM plan-view images showing a time interrupted growth series of PbS films deposited at 30°C for 5, 15 and 30 min from the initiation of the reaction in presence of (a-c) 0 mM and (d-f) 17 mM citrate.

The fact that the cluster mechanism is favoured with the retarded growth rate in presence of citrate is evidenced from the formation of the cube-like PbS nanocrystals in presence of the citrate. It has been reported that at low deposition rates (with sufficient thermal energy and a low flux of reactants), controlled growth results in the most stable shapes of the film grains such as cube-shaped grains in the rocksalt phase[20,21]. The grains in the initial nucleation of PbS film appear to have rounded shape as can be seen in Figures 9e and 10a, and then develop into shapes that are terminated by (111) and (100) facets, and their relative stability determines the final shape of the nanocrystal[20]. The facets usually develop during the ion-by-ion growth mechanism. After the initial film formation through cluster mechanism, there is a transition to the ion- by-

CrystEngComm Accepted Manuscript

ion mechanism in which these initial clusters transform into faceted nano-cubes. In rocksalt structures, the (111) surface typically has a higher surface energy and hence in a thermodynamically driven regime, there is a faster growth on the (100) facets favouring the formation of cube shaped PbS nanocrystals. In presence of the citrate, the effective complexation of Pb^{2+} results in the low supply of free metal cations, resulting in the thermodynamically driven regime which in turn results in the cube shaped PbS nanocrystals.

To quantify the slower growth rate in presence of citrate, the initial formation of the PbS clusters in solution was monitored in real time using UV-vis absorption under different deposition conditions and the resulting spectra are showed in Figure 11. Interestingly, before the addition of TU, the last reagent to initiate the reaction, there is a peak at ~300 nm for solutions containing Pb^{2+} ions and NaOH (similar with or without citrate). This peak corresponds to the formation of various Pb-OH complexes as described by Hodes *et al.*[17] However, the peak intensity and position are unaffected by the presence of citrate, indicating that –OH remains the dominating complexing agent and citrate is acting as a co-complexant at this relatively high pH. This well-defined peak at 300 nm is replaced by a strong absorption edge with an onset at ~330 nm immediately after thiourea addition and initiation of the reaction. At lower temperature, 20°C, with time there a new peak emerging at ~400 nm which is further red shifted with time to ~600 nm, indicating growth of the initial PbS clusters in suspension. The walls of the absorption cuvette were found to be not absorbing in this region indicating that film formation on the quartz cuvette in negligible and that these results are due to absorption of the PbS clusters formed in the solution itself. Estimating the possible sizes from the band gap calculation[22] reveals formation of ultra-small PbS nanoclusters with the sizes ranging from ~2-3 nm which ripen in size with time. In presence of citrate at the same temperature, the peak growth is much slower, showing that within the same time interval of 20 min, the peak remains at 400 nm without further red shift. At 30°C, in absence of citrate, the peak appears much faster (after 1 min) and rapidly red-shifts towards the near infrared region. Interestingly, after 10 min from initiation of the reaction, the peak at 400 nm re-appears and again, red shifts with time, probably indicating a second phase of nucleation in solution. In the presence of citrate at 30°C, the red shifting of the peak is much slower, with the peak shifting to 700 nm for the same interval of time (10 min).

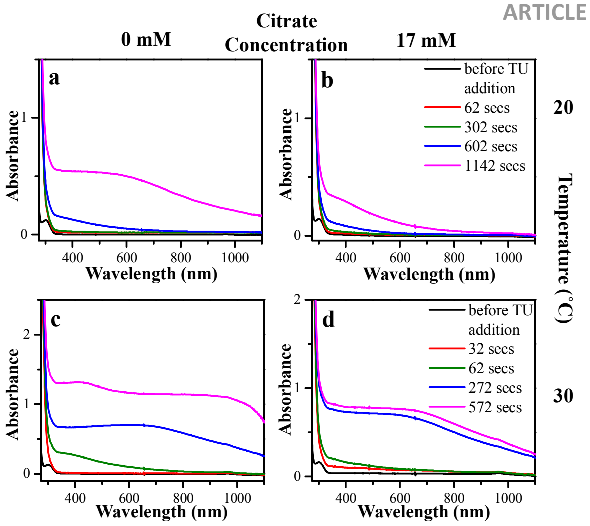

Figure 11. Real-time UV-Vis spectra obtained *in-situ* during the initial stage of PbS formation at two different temperatures (a,b) 20˚C and (c,d) 30˚C with 0 mM (a,c) and 17 mM (b,d) citrate concentrations. The time in the legends denotes the time elapsed from TU addition. The legend in b applies also for a. The legend in d applies also for c.

This rate of formation of PbS can be quantified by plotting the rate of change in absorbance at a particular wavelength with time at different temperatures (Figure 12 a,b). This rate of change can be fitted with a straight line indicating a zero-order reaction. For growth through cluster mechanism, the rate determining step is supposed to be the decomposition of the metal-complex on the substrate with the rates independent of the concentrations of both Pb and TU while for ion-by-ion mechanism, the rate is found to be directly dependent on reaction between the metal ion and the sulfide ions onto the substrate. Thus, occurrence of zero-order reaction indicates the presence of cluster mechanism. The line fitting provides the corresponding growth rate (r) which can be subsequently used for constructing Arrhenius plots, showing inverse exponential dependence of the growth rate with temperature (Figure 12c). The Arrhenius plot presents an evaluation of the activation energies of the reaction in presence and absence of citrate. The activation energy for the formation of PbS in absence of citrate has been found to be 19±2 kcal/mole. With the presence of citrate, the activation energy was found to substantially increase to 30±3 kcal/mole. This quantitatively reflects the much slower formation of PbS clusters in presence of citrate in solution, due to the effective complexation of the Pb^{2+} ion.

CrystEngComm Accepted Manuscript

Please do not adjust margins

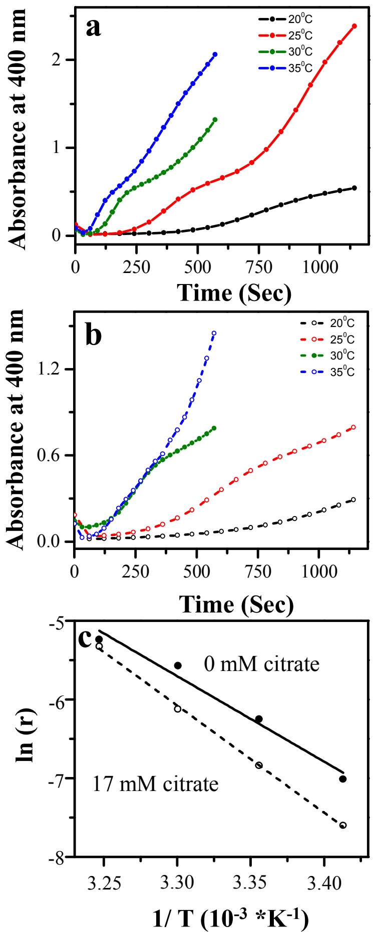

Figure 12. Absorbance at 400 nm plotted vs. time, as obtained from the UV-vis spectra at different temperatures in presence of (a) 0 mM and (b) 17 mM citrate concentrations. (c) Arrhenius plots. The curves were fitted to obtain the rate (r) which is plotted vs. 1/temperature in °K. The straight lines indicate the best linear fit.

From the results obtained so far it has been shown that the introduction of citrate results in a significant decrease in particle size which can be expected to affect the optical properties of the films[23-25]. The ability to tune the optical properties of lead chalcogenide thin films has been of considerable interest for advanced optoelectronic applications such as short wave infrared night vision systems, etc. We note that band gap values obtained from PL measurements are straightforward and accurate compared to those obtained from the IR transmission measurements which must be corrected for reflectance and depend on surface quality. The previous HRSEM images show the formation of three different sizes of PbS under different experimental conditions. At 30°C and 13.2 pH bulk PbS is formed in absence of citrate. Decreasing the temperature to 20°C, in presence of 17 mM citrate PbS nanocubes with dimensions of ~100 nm are formed and further decreasing the pH to 12.9 results in the formation of nanocubes with the dimension of ~20-50 nm. The PL measurements obtained for these three different PbS films are depicted in the following figure (Figure 13d).

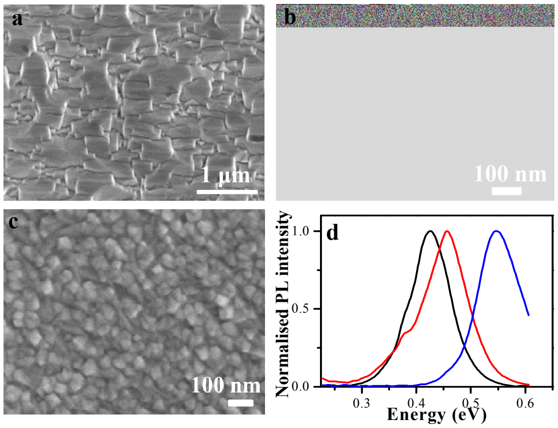

Figure 13. HRSEM plan-view images obtained at different deposition conditions to yield different sizes of PbS nanocrystals. (a) bulk PbS (b) PbS nanocubes with dimensions ~100 nm (c) PbS nanocubes with dimensions in the range ~20-50 nm. (d) The corresponding PL spectra. The black, red and blue curves correspond to the SEM images in (a), (b) and (c) respectively.

The optical properties of the PbS has been studied by various groups previously which suggested a hyperbolic model to explain the band gap dependence on particle size[26-29]. Our PL spectra indicate a significant blue shift from the bulk value depending on the size of the PbS nanocrystals, showing a clear trend of increasing band gap energy with decreasing grain sizes. We note that it is quite surprizing that quantum size effects are observed already for the 100 nm nanocube sample, suggesting either that (i) the bulk of the film is comprised of grains that are substantially smaller than those observed with HRSEM on the sample surface. (ii) the individual nanocubes are comprised of sub-domains that are separated by confining boundaries. These results indicate that realization of size tunable band gap properties of the PbS nanocrystals can be easily achieved by using citrate bath additives under moderate growth temperatures and relatively short deposition periods. Earlier studies reported that nanocrystalline PbS could only be achieved at extremely low bath temperatures (close to 0°C) and for significant long deposition time (over 24 hours).[30]

Conclusions

We conclude that the citrate acting as co-complexant for the Pb^{2+} cations has a prominent effect on CD of PbS thin films. For the conditions favouring film growth via cluster mechanism, the presence of citrate slows down the reaction of PbS formation, with strong texturing along the (100) direction and the formation of cube-shaped PbS nanocrystals. The slower growth rate in presence of citrate has been confirmed using HRSEM and XRD coupled with *in-situ* light scattering and UV-vis absorption spectroscopy for real time monitoring of

CrystEngComm Accepted Manuscript

This journal is © The Royal Society of Chemistry 20xx

Please do not adjust margins

deposition. Calculations indicate a substantial increase of ~10 kcal/ mole in activation energy in presence of citrate which results in retardation of the rate of cluster formation in solution. Upon increasing temperature and pH, the ion-by-ion mechanism becomes dominant and citrate has less effect on the deposition and on the resulting film morphology. The slower growth rate during film growth via cluster mechanism leads to significant decrease in grain size of the films, and subsequently, to a blue shift in the film bandgap. Apart from acting as co-complexant, the citrate additive appears to act also as a surface active agent, stabilizing smaller PbS grain size which can be obtained at moderate growth conditions. This trend in decreasing PbS nanocrystal size and its manifestation in corresponding increase in band gap energy, provides additional means of control for future use of size quantized films in advanced optoelectronic applications.

Acknowledgements

We thank Dr. Dmitry Mogilyansky for expert assistance in XRD, Dr. Sharon Hazan for expert assistance in LS measurements and Prof. Ira Weinstock for providing access to their UV-vis spectrometer. This work was funded by the Israel Science Foundation under Grant #156/14, and by the Focal Technological Area (FTA) program of the Israeli National Nanotechnology Initiative (INNI). S.S.G acknowledges a postdoctoral fellowship from the Planning and Budgeting Committee of the Israeli Council for Higher Education.

Notes and references

1 Hodes, G., Marcel Dekker, Inc.: New York, 2002.
2 Bose, J. C. U.S. Patent, 755, 840, 1904.
3 Nair, P. K.; Nair, M. T. S.; Fernandez, A.; Ocampo, M., J. Phys. D: Appl. Phys. 1989, 22, 829.
4 4. Nair, P. K.; Nair, M. T. S., J. Phys. D: Appl. Phys. 1990, 23, 150.
5 Kumar, D.; Agarwal, G.; Tripathi, B.; Vyas, D.; Kulshrestha, V., J. Alloys Compd. 2009, 484, 463.
6 Seghaier, S.; Kamoun, N.; Brini, R.; Amara, A. B., Mater. Chem. Phys. 2006, 97, 71.
7 Osherov, A.; Ezersky, V.; Golan, Y., J. Cryst. Growth 2007, 308, 334.
8 Osherov, A.; Golan, Y., Mater. Res. Soc. Bulletin 2010, 35, 790.
9 Osherov, A.; Ezersky, V.; Golan, Y., Eur. Phys. J. Appl. Phys. 2007, 37, 39.
10 Gode, F.; Guneri, E.; Baglayan, O., Appl. Surf. Sci. 2014,318, 227.
11 Agawane, G. L.; Shin, S. W.; Moholkar, A. V.; Gurav, K. V.; Yun, J. H.; Lee, J. Y.; Kim, J. H., J. Alloys Compd. 2012,535, 53.
12 Yucel, E.; Yucel, Y.; Beleli, B., J. Alloys Compd. 2015,642, 63.
13 Sadovnikov, S. I.; Gusev, A. I., J. Alloys Compd. 2014,586, 105.
14 Pawar, S. B.; Shaikh, J. S.; Devan, R. S.; Ma, Y. R.; Haranath, D.; Bhosale, P. N.; Patil, P. S., Appl. Surf. Sci. 2011, 258, 1869.
15 Bobtelsky, M.; Graus, B., J. Am. Chem. Soc. 1953, 75, 4172.
16 Gorer, S.; Hodes, G., J. Phys. Chem. 1994, 98, 5338.
17 Gorer, S.; Albu-Yaron, A.; Hodes, G., Chem. Mater. 1995, 7, 1243.
18 Shandalov, M.; Golan, Y., Chem. Mater. 2006, 18, 3593.
19 Tanford, C., Physical Chemistry of Macromolecules. John Wiley & Sons, Inc.: New York, 1961.
20 Lee, S. M.; Cho, S. N.; Cheon, J., Adv. Mater. 2003, 15, 441.
21 Xiong, Y.; Xia, Y., Adv. Mater. 2007, 19, 3385.
22 Moreels, I.; Lambert, K.; Smeets, D.; De Muynck, D.; Nollet, T.; Martins, J. C.; Vanhaecke, F.; Vantomme, A.; Delerue, C.; Allan, G.; Hens, Z., ACS Nano 2009, 3, 3023.
23 Gutman, N.; Armon, A.; Sa'ar, A.; Osherov, A.; Golan, Y., Appl. Phys. Lett. 2008, 93, 073111.
24 Gutman, N.; Armon, A.; Shandalov, M.; Osherov, A.; Golan, Y.; Sa'ar, A., J. Nanosci. Nanotechnol., 2009, 9, 3648.
25 Gutman, N.; Armon, A.; Osherov, A.; Golan, Y.; Sa'ar, A., Phys. Status Solidi (a) 2009, 206, 1290.
26 Nosaka, Y., J. Phys. Chem. 1991, 95, 5054.
27 Wang, Y.; Suna, A.; Mahler, W.; Kasowski, R., J. Chem. Phys. 1987, 87, 7315.
28 Valenzuela-Jauregui, J. J.; Rami rez-Bon, R.; Mendoza-Galvan, A.; Sotelo-Lerma, M., Thin Solid Films 2003, 441, 1104
29 Joshi, R. K.; Kanjilal, A.; Sehgal, H. K., Appl. Surf. Sci. 2004, 221, 143.
30 Safrani, T.; Kumar, T. A.; Klebanov, M.; Arad-Vosk, N.; Beach, R.; Sa'ar, A.; Abdulhalim, I.; Sarusi, G.; Golan, Y., J. Mater. Chem. C 2014, 2, 9132.

CrystEngComm Accepted Manuscript